

# An Application of Computerized Axial Tomography (CAT) Technology to Mass Raid Tracking

By

John K. Barr

August 1989

Prepared for

Program Director for Airborne Warning and Control Systems

Electronic Systems Division

Air Force Systems Command

United States Air Force

Hanscom Air Force Base, Massachusetts



Approved for public release;  
distribution unlimited.

Project No. 411A

Prepared by

The MITRE Corporation

Bedford, Massachusetts

Contract No. F19628-89-C-0001


ADA214401

When U.S. Government drawings, specifications or other data are used for any purpose other than a definitely related government procurement operation, the government thereby incurs no responsibility nor any obligation whatsoever; and the fact that the government may have formulated, furnished, or in any way supplied the said drawings, specifications, or other data is not to be regarded by implication or otherwise as in any manner licensing the holder or any other person or conveying any rights or permission to manufacture, use, or sell any patented invention that may in any way be related thereto.

Do not return this copy. Retain or destroy.

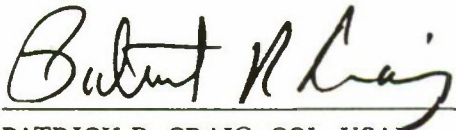
### REVIEW AND APPROVAL

This technical report has been reviewed and is approved for publication.



RICHARD E. BUCK, GS-13  
ESMS Engineer

FOR THE COMMANDER



PATRICK R. CRAIG, COL, USAF  
Program Director  
Airborne Warning and Control Systems

**UNCLASSIFIED**

SECURITY CLASSIFICATION OF THIS PAGE

**REPORT DOCUMENTATION PAGE**

1a. REPORT SECURITY CLASSIFICATION Unclassified			1b. RESTRICTIVE MARKINGS		
2a. SECURITY CLASSIFICATION AUTHORITY			3. DISTRIBUTION / AVAILABILITY OF REPORT Approved for public release; distribution unlimited.		
2b. DECLASSIFICATION / DOWNGRADING SCHEDULE					
4. PERFORMING ORGANIZATION REPORT NUMBER(S) MTR-10542 ESD-TR-89-305			5. MONITORING ORGANIZATION REPORT NUMBER(S)		
6a. NAME OF PERFORMING ORGANIZATION The MITRE Corporation		6b. OFFICE SYMBOL (if applicable)		7a. NAME OF MONITORING ORGANIZATION	
6c. ADDRESS (City, State, and ZIP Code) Burlington Road Bedford, MA 01730			7b. ADDRESS (City, State, and ZIP Code)		
8a. NAME OF FUNDING / SPONSORING ORGANIZATION Program Director (continued)		8b. OFFICE SYMBOL (if applicable) ESD/TCWD-1		9. PROCUREMENT INSTRUMENT IDENTIFICATION NUMBER F19628-89-C-0001	
8c. ADDRESS (City, State, and ZIP Code) Electronic Systems Division, AFSC Hanscom AFB, MA 01731-5000			10. SOURCE OF FUNDING NUMBERS		
			PROGRAM ELEMENT NO.	PROJECT NO. 411A	TASK NO.
11. TITLE (Include Security Classification) An Application of Computerized Axial Tomography (CAT) Technology to Mass Raid Tracking					
12. PERSONAL AUTHOR(S) Barr, John K.					
13a. TYPE OF REPORT Final		13b. TIME COVERED FROM _____ TO _____		14. DATE OF REPORT (Year, Month, Day) 1989 August	
15. PAGE COUNT 27					
16. SUPPLEMENTARY NOTATION					
17. COSATI CODES			18. SUBJECT TERMS (Continue on reverse if necessary and identify by block number) Computerized Axial Tomography (CAT) Scanner Electronic Support Measures (ESM) Fusion (continued)		
FIELD	GROUP	SUB-GROUP			
19. ABSTRACT (Continue on reverse if necessary and identify by block number) <p>This paper outlines a new technique for performing surveillance in mass raid scenarios using information from passive sensors such as Electronic Support Measures (ESM). In a high target density environment, cooperative passive tracking may not be possible. Instead of individual target tracks, the method described here generates a Target Density Map (TDM) with estimates of the number of targets in each of many small grid cells covering the surveillance area. Target Density Reconstruction is similar to image reconstruction in a computerized axial tomography (CAT) scanner.</p> <p>This paper was presented at the 1988 Tri-Service Data Fusion Symposium held at the Johns Hopkins Applied Physics Laboratory.</p>					
20. DISTRIBUTION / AVAILABILITY OF ABSTRACT <input type="checkbox"/> UNCLASSIFIED/UNLIMITED <input checked="" type="checkbox"/> SAME AS RPT. <input type="checkbox"/> DTIC USERS			21. ABSTRACT SECURITY CLASSIFICATION Unclassified		
22a. NAME OF RESPONSIBLE INDIVIDUAL Pamela J. Cunha			22b. TELEPHONE (Include Area Code) (617) 271-2844		22c. OFFICE SYMBOL Mail Stop D135

**UNCLASSIFIED**

**UNCLASSIFIED**

8a. for Airborne Warning and Control Systems

18. High Target Density  
Passive Tracking  
Surveillance

**UNCLASSIFIED**

#### ACKNOWLEDGMENT

This document has been prepared by The MITRE Corporation under Project No. 411A, Contract No. F19628-89-C-0001. The contract is sponsored by the Electronic Systems Division, Air Force Systems Command, United States Air Force, Hanscom Air Force Base, Massachusetts 01731-5000.

## PREFACE

This paper was presented at the 1988 Tri-Service Data Fusion Symposium (DFS-88), which was held at Johns Hopkins University Applied Physics Laboratory in Laurel, MD, from 17 to 19 May 1988.

DFS-88 was the second annual symposium intended to provide a forum for the broad exchange of information and ideas on the development of data fusion technology for Department of Defense applications. The theme of this year's symposium was the role of data fusion in tactical command and control (C<sup>2</sup>).

The symposium was organized under the auspices of the Joint Directors of Laboratories, Data Fusion Subpanel, and sponsored by CECOM Center for Signals Warfare, Naval Air Development Center, Naval Ocean Systems Center, and Rome Air Development Center. The symposium was limited to United States citizens only and was attended by approximately 500 representatives from Government and industry.

The discussion ranged over the data fusion spectrum and included sessions on operational C<sup>2</sup> issues, commanders' tactical C<sup>2</sup> perspectives, and joint service issues in addition to the technical presentations. This paper was presented in the Advanced Concepts session.



## TABLE OF CONTENTS

SECTION	PAGE
1 Introduction . . . . .	1
2 Rationale . . . . .	2
3 Target Density Reconstruction Processing . . . . .	7
Sorting of Signals into Subgroups . . . . .	7
Density Reconstruction . . . . .	7
Implementation of Density Reconstruction . . . . .	12
4 Target Density Map Examples . . . . .	15
5 Conclusion . . . . .	18
List of References . . . . .	19

## LIST OF ILLUSTRATIONS

FIGURE	PAGE
1 Mass Raid Target Locations . . . . .	3
2 Strobes at Three ESM Sites . . . . .	4
3 Target Density Map True Densities . . . . .	6
4 Sector Equation . . . . .	8
5 Sampling in Density Reconstruction . . . . .	14
6 Target Density Map: Reconstructed Densities . . . . .	16
7 Target Density Map: Reconstructed Densities (9 Groups). . . . .	17



## SECTION 1

### INTRODUCTION

In this paper we discuss a new technique, Target Density Reconstruction, for using passive angle-only data from multiple sensor sites to derive the location of large numbers of airborne targets. In a high target density, intense jamming environment, the tracking of individual targets by radar may be severely degraded, and passive sensors such as Electronic Support Measures (ESM) may provide the only target data. Cooperative passive tracking using ESM data may itself be difficult when many targets are present. The Target Density Reconstruction method described here is designed to gain the maximum possible raid location information from passive data. Instead of individual target tracks, it generates a Target Density Map (TDM) with estimates of the number of targets in each of many small grid cells covering the surveillance area. Target Density Reconstruction is similar to image reconstruction in a Computerized Axial Tomography (CAT) scanner.

## SECTION 2

### RATIONALE

Target Density Reconstruction is a means of deriving the maximum amount of summary raid location information when standard tracking from radar has been degraded and ESM cooperative tracking is not possible due to the great number of emitter signals present in the environment. Target Density Reconstruction is intended as a backup to the radar and ESM tracking which would be used in less dense emitter environments.

The scenario for use of Target Density Reconstruction is a massive air attack with hundreds of aircraft in multiple waves crossing a border in one or more corridors. The invading aircraft are protected by jamming of the defending radars. Figure 1 shows the locations of aircraft several minutes into a generic raid of this type. The Dense Raid environment is described in detail in reference 1. The intense jamming during the raid could seriously degrade the ability to radar track individual aircraft.

We assume that a netted system of ESM sensors is in place, such that any potential aircraft location is in line of sight to at least three ESM sites. Each ESM system can detect and measure the radar and other signals being emitted by the aircraft in its field of view. The azimuth Angle of Arrival (AOA) to each target at each ESM site is determined, along with signal parameters such as Radio Frequency (RF) and Pulse Repetition Interval (PRI).

With a small number of targets it is generally possible to combine the AOAs measured at two ESM sites to triangulate a target, and to perform cooperative passive tracking. However, this form of tracking requires correct association of the angle strobe at one ESM site with the strobe generated by the same emitter target at the other ESM site. With  $N$  targets to be tracked,  $N$  strobes will be generated at each of two ESM sites, leading to  $N^2$  strobe crossings. Each crossing is a possible target location, but only  $N$  of them are correct. The remaining  $N^2 - N$  crossings are called "ghosts." With data from three sites, the ghosting problem can be even worse -- on the order of  $N^3$  crossings generated. Figure 2 shows the strobe pattern produced at three passive sensor sites by the Dense Raid shown in figure 1.

In less dense target situations, the ESM signal measurements can be used to sort out the valid strobe pairings. But with the large number of targets being postulated here, signals from different emitters may overlap in their measured parameters, becoming indistinguishable to the ESM system. Emitters may also change their operating characteristics between the time of detection at one ESM site to the time of detection at another, making cross-correlation difficult or impossible. For example, the ESM system may detect a signal once each 10 or more seconds, while the target emitter is



Figure 1. Mass Raid Target Locations



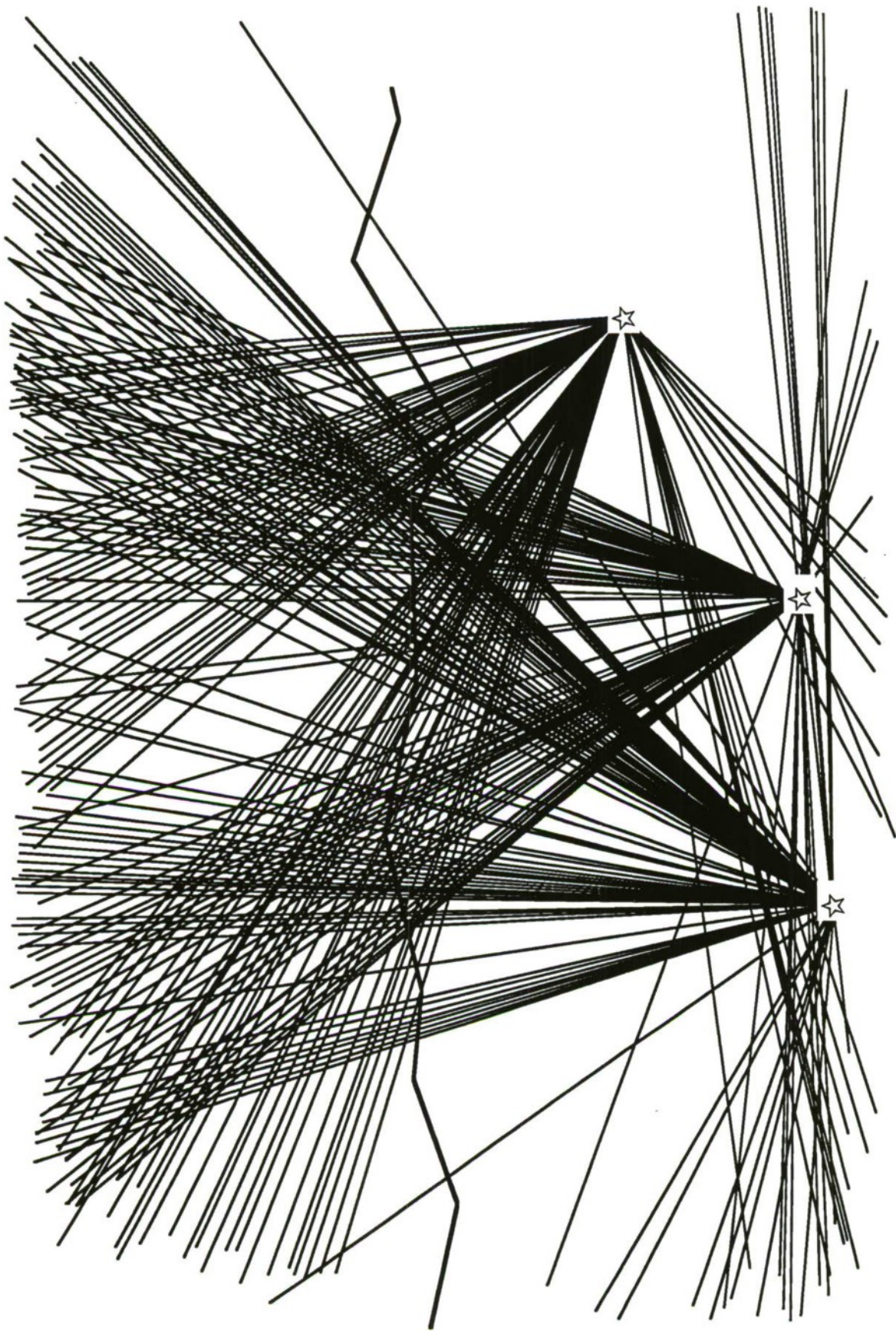
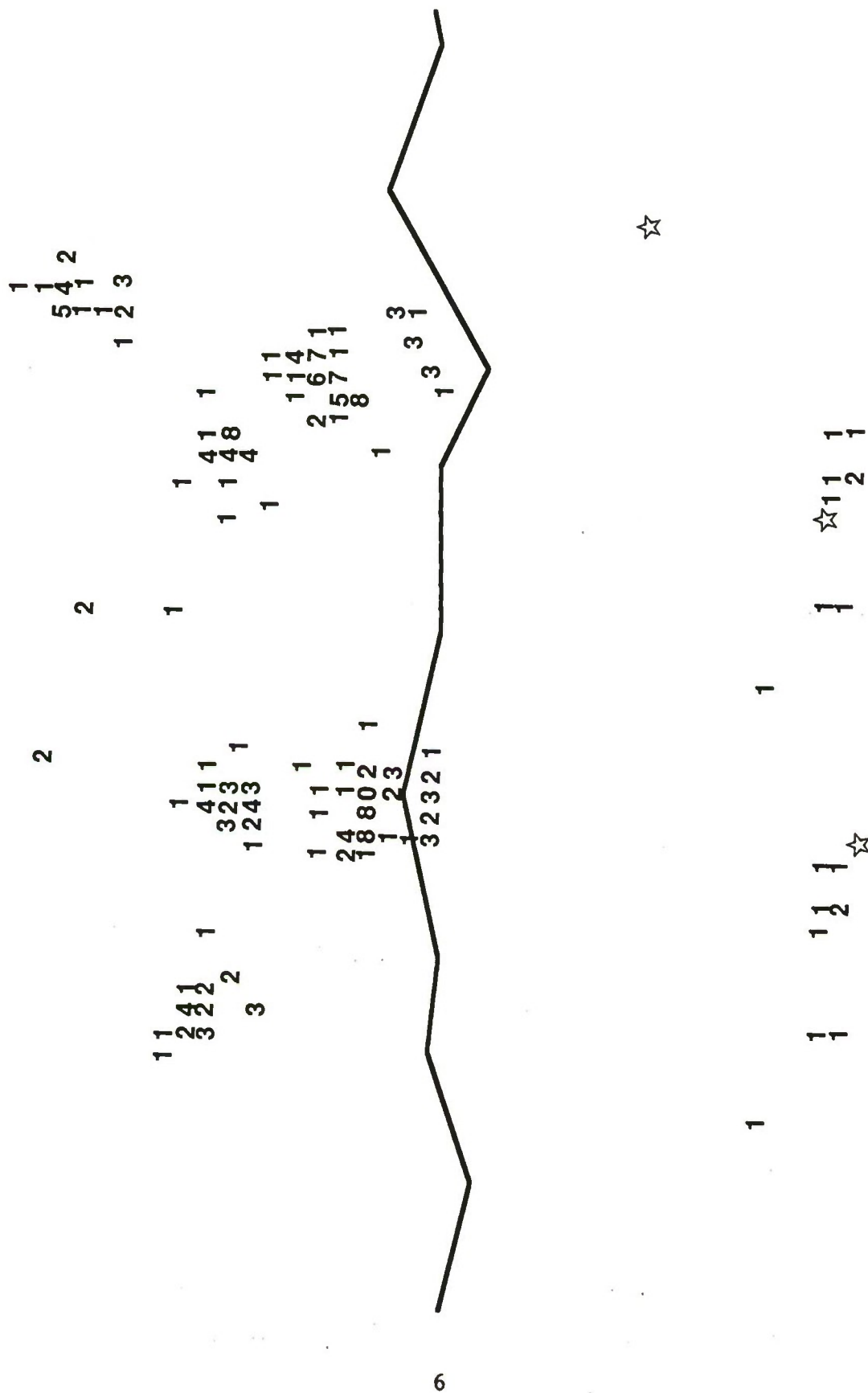


Figure 2. Strobes at Three ESM Sites

changing RF and/or PRI many times a second. For these reasons, cooperative tracking by ESM sites may be degraded in a dense raid environment.

The method of Target Density Reconstruction is intended to fill the gap left by the missing radar and cooperative passive trackers, by providing an estimate of the general raid situation in as much detail as possible. Although individual tracks are not derived, the Target Density Map gives an estimate of the number of targets in each 10 km by 10 km grid cell. Figure 3 shows a TDM generated directly from the true target locations given in figure 1. The goal of an estimated TDM using ESM measurement data would be to come as close as possible to figure 3. The accuracy of the estimated TDM depends on the number of ESM sites measuring the grid cell and also on the accuracy of the ESM system's measurements of AOA and signal parameters.





## SECTION 3

### TARGET DENSITY RECONSTRUCTION PROCESSING

#### SORTING OF SIGNALS INTO SUBGROUPS

The use of ESM data for target location depends critically upon the ability of the ESM system to discriminate between emitters based on signal characteristics. When signal features are measured and data from different ESM sites are combined, reports with identical signal parameter values can be processed as a separate group. This breaks up one large data association problem into many smaller such problems, each of which can be more easily solved. The ideal, of course, would be to have only one ESM report per site in a group, which allows for cooperative tracking. If the number of targets in the group is small enough, relative to the angular resolution of the ESM, discrete tests can eliminate many ghost intersections. The principal test rejects a strobe intersection from two ESM sites which is not corroborated by a strobe from a third site. Other more complicated tests can be employed, but are not discussed in this paper.

#### DENSITY RECONSTRUCTION

Target Density Reconstruction is an application to ESM data of the general Density Reconstruction technique which has been successfully applied in such fields as radio astronomy and Computerized Axial Tomography (CAT) scanning [2], [3]. The technique is basically a way of recreating the distribution of the contents of a region when all that is known about the region are the sums of that content along lines through it. There are two essential input requirements which must be satisfied for Density Reconstruction to work in the target problem. The first, which can be satisfied by ESM systems, but not by some other passive systems, is that the number of emitters be counted along each angle of arrival. The second requirement is that ESM data be available from at least three sites. The count data from only one site is not enough to perform any reconstruction, and two-site reconstruction is not generally useful. Once data from three or more sites is combined, however, Density Reconstruction can give a good picture of emitter location densities.

We now describe the computation method and apply it to the case of a Dense Raid scenario with ESM data. We also point out features of the Dense Raid/ESM problem that make ESM Density Reconstruction different from that in a CAT scanner or other typical applications. We will concentrate on the case of three sites. Processing is similar when more sites are present.

In the ESM Density Reconstruction problem the inputs are the number of emitters detected in each angular sector, for all the cooperating sites. Examine, for example, the  $i$ th sector with respect to site A (see figure 4). The borders of sectors centered on other sites cut across sector  $i$  and



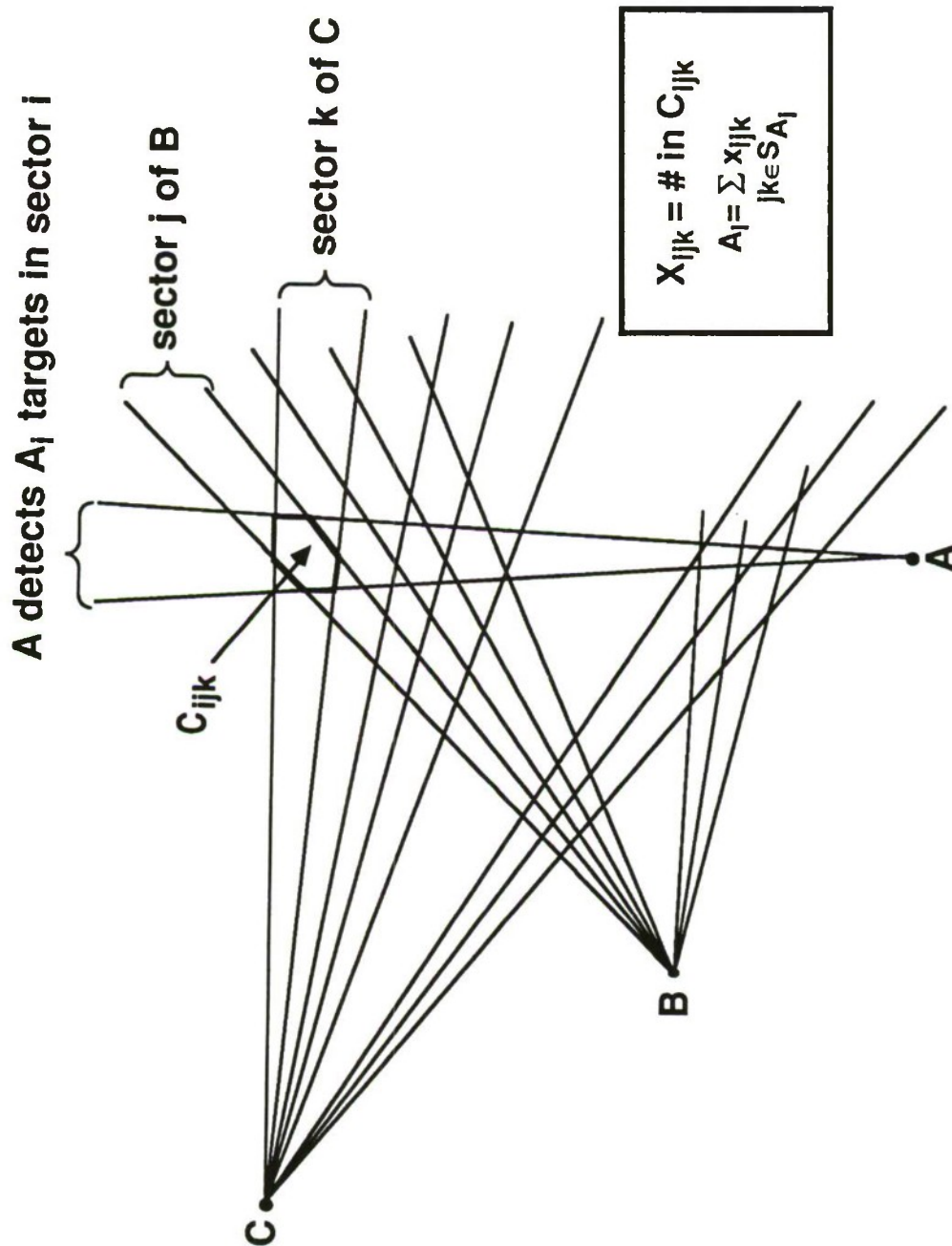


Figure 4. Sector Equation

divide it into many small odd-shaped pieces,  $C_{ijk}$ , called calculation cells. Here,  $C_{ijk}$  is the calculation cell cut out by sector  $i$  from  $A$ , sector  $j$  from  $B$  and sector  $k$  from  $C$ . If  $X_{ijk}$  is the number of targets in the calculation cell  $C_{ijk}$ , and site  $A$  has measured  $A_i$  targets in sector  $i$ , then

$$A_i = \sum_{(j,k) \in S_{Ai}} X_{ijk} \quad (1)$$

In the equation  $S_{Ai}$  is the set of pairs  $(j,k)$  such that  $C_{ijk}$  is a calculation cell in sector  $i$  of site  $A$ . Each sector defines one such equation relating calculation cell target counts to an angle sector count. The technique of Density Reconstruction is to solve for the  $X_{ijk}$ 's using all sector equations (1) for all sites. If there are three sites and  $n$  angle sectors about each site, this means that  $3n$  equations are defined. Only  $3n-2$  of the equations are independent, and there are, in general, many more than  $3n-2$  calculation cell unknowns  $X_{ijk}$ , so the system of equations (1) is badly underdetermined.

Three steps are used in ESM Density Reconstruction to reduce the size of the problem and find a reasonable solution. The first is to notice that, being a count of targets,  $X_{ijk}$  could not be negative. Thus, the  $X_{ijk}$ 's must then not only satisfy (1) but also

$$X_{ijk} \geq 0 \quad \text{for all } X_{ijk} \quad (2)$$

This step reduces the number of possible solutions, but does not provide a unique one.

The second and critical step uses the fact that many angle sectors contain no emitters at all, even in a Dense Raid scenario. If a platform emitter count is zero in a sector, then all the calculation cells in the sector must be empty of emitters, and their  $X_{ijk}$ 's must be zero. These  $X_{ijk}$ 's and the sector equation can now be eliminated from further processing. Since many  $X_{ijk}$ 's are eliminated and only one equation is lost, this step improves the balance of equations against unknowns as well as reduces the computational load. If the ESM system has been able to divide the strobe data into several smaller data sets, then the improvement from step 2 is even sharper than when all strobes are processed together. This is because fewer targets and AOA reports allow for additional elimination of calculation cells.

Even after steps 1 and 2 the system defined by equations (1) and (2) is still badly underdetermined, with no unique solution. The problem is then to find the best solution from among many possible ones, on the basis that even if that solution does not exactly match the true emitter

locations, it will be close enough to be useful. Two criteria have been proposed frequently as ways to select a best solution. Each algorithm is implemented in the real number system, with results rounded later for display. The first, called the Algebraic Reconstruction Technique (ART), is an iterative quadratic optimization which converges to the smoothest solution, i.e., the one that minimizes

$$\sum_{ijk} (X_{ijk} - X)^2 \quad (3)$$

where  $X$  is the average value over all the  $X_{ijk}$ . See reference 3 for details on ART. An update generated by ART does not automatically satisfy the non-negativity constraint (2) on the solution. This constraint can be explicitly coded into the iteration by setting to zero those  $X_{ijk}$  that would otherwise be set to negative values. ART was the algorithm used in the first commercial CAT scanner, but has given consistently poor results in ESM and in the study [4], where three-view reconstruction methods were compared.

The second criterion for choosing a best density solution from the set of possible solutions used a probabilistic approach to choose a maximum likelihood solution. The reasoning of Jaynes in reference 5 is applied to the target problem as follows.

Suppose there are  $N$  calculation cells and a total of  $R$  aircraft. We make the simplifying assumption that any "configuration" or specific placement of aircraft into the cells is equally probable. This assumption corresponds to not knowing the prior probabilities. There are  $N^R$  configurations, and each configuration generates a particular density solution  $\{X_{ijk}\}$ , where, as above,  $X_{ijk}$  is the count in cell  $C_{ijk}$ . The number of configurations having the same density  $\{X_{ijk}\}$  is the multiplicity

$$W = \frac{R!}{\prod_{ijk} (X_{ijk}!)} \quad (4)$$

Since we assume that each configuration is equally probable, the likelihood of a given density solution  $\{X_{ijk}\}$  can be directly calculated, since it is just the multiplicity  $W$  of configurations having that density divided by the total number  $N^R$  of configurations, i.e.,

$$\text{Prob}(\{X_{ijk}\}) = W/N^R \quad (5)$$

The target density algorithm then seeks the maximum likelihood density solution over all densities that satisfy the ESM measurement constraint equations. As usual in maximum likelihood estimation, it is convenient to solve for the maximum logarithmic likelihood solution. Since in a given



reconstruction the numbers  $N$  and  $R$  are fixed and known, the maximum likelihood solution occurs at the maximum of  $\ln(W)$ . In reconstruction, the number  $R$  of aircraft is large, allowing use of Stirling's approximation for  $R!$ , to give

$$\ln(W)/R = - \sum_{ijk} (X_{ijk}/R) \ln (X_{ijk}/R) \quad (6)$$

Since the sum on the right is the entropy  $H(\{X_{ijk}\})$  of the vector of numbers  $\{X_{ijk}\}$ , maximizing  $\ln(W)$  is equivalent to the well-known Maximal Entropy solution to the ESM angle sector equations. With  $K$  measurement constraint equations, the distribution of configurations near the Maximal Entropy solution is shown by the Entropy Concentration Theorem [5] to be chi-squared with  $k = N - K - 1$  degrees of freedom. Thus for large  $R$ , the fraction  $F$  of configurations having entropy within  $\Delta H$  of the peak value is given by

$$2R \Delta H = \chi_k^2 (1 - F) \quad (7)$$

Since we assume that each configuration has the same probability, this expression then can give an estimate of their distribution near the Maximal Entropy peak.

The Maximal Entropy solution is easily found by using the MENT iteration algorithm, which converges to the unique entropy peak. It can be shown [6] that the  $X_{ijk}$  in a Maximal Entropy solution have the form of products

$$X_{ijk} = E_i E_j E_k \quad (8)$$

where  $E_i$ ,  $E_j$ , and  $E_k$  are intermediate variables defined for each sector. Then each sector equation can be written

$$A_i = \sum_{(j,k) \in S_{Ai}} X_{ijk} = \sum_{(j,k) \in S_{Ai}} E_i E_j E_k = E_i \sum_{(j,k) \in S_{Ai}} E_j E_k \quad (9)$$

and a solution must satisfy

$$E_i = \frac{A_i}{\sum_{(j,k) \in S_{Ai}} E_j E_k} \quad (10)$$

In the MENT iteration algorithm, each equation (10) is used in turn to update the value of a single  $E_i$  from the current values of the  $E_j$  and  $E_k$ . The unknowns  $E_i$ ,  $E_j$ , and  $E_k$  are initialized to 1. After three to five cycles through the entire set of sector equations, the  $E$ 's are changing by small increments, and the iterations are ended. The output  $X_{ijk}$  are then generated from equation (8). With 185 targets, the MENT algorithm required from 10 to 20 seconds to reconstruct target TDMs on a VAX 11/750 system.

The Density Reconstruction algorithm can be summarized as a setup stage, in which a minimal number of unknowns is found, and a second phase in which the linear equations relating the unknowns to the data are iteratively solved. Since the variables  $X_{ijk}$  refer to odd-shaped calculation cells in the surveillance region, some of them quite small, the resulting solution must be translated to a regular grid before being given to the user. This is done by adding together the densities of the calculation cells contained in a grid box and integerizing the result for output. If a cell has parts in different grid boxes, its calculated density is prorated among the boxes according to area.

#### IMPLEMENTATION OF DENSITY RECONSTRUCTION

The two main parts of Target Density Reconstruction are the definition of the unknown densities to be calculated and the iterative solution for them. We now examine the different approaches that can be taken to implement the density equations and unknowns and the reasoning that has led to the present algorithm.

The most difficult part of Density Reconstruction is the definition of the variables  $X_{ijk}$  and their equations. This step is quite simple in CAT scanners and other applications of the technique, where a fixed 2-dimensional grid is used to define the areas whose densities must be calculated. In ESM Density Reconstruction such grids have given poor results, leading to the use instead of calculation cells described above.

The problem with using a grid to define the unknowns in ESM Density Reconstruction is that it cannot accurately represent the reconstruction geometry near the ESM sites. For example, if a sector angle size of 1 degree is used, then a 1 km grid size is adequate for areas further than 57 km from any site. A grid cell closer than this will not be contained in a single sector centered at the site so its variable  $X$  must be allocated to more than one sector equation, leading to inconsistent equations. To overcome this sampling problem, variable size grids were tried, but these were found to be very computationally expensive, as well as producing large numbers of variables.

The method that we used replaces square grids with more general angle-sector sampling. In the grid definition processing, a coarse grid of equilateral triangles 50 km on a side covering the surveillance area (excluding points near the ESM sites) is scanned. For each coarse grid

point X, sectors from all platforms intersecting the region near X are checked. If none of these sectors has a positive emitter count, then the region is empty and is dropped from further processing. Otherwise, a fine grid is set up near X in the following way. Referring to figure 5, suppose that Site B is closest to X. Then the midlines of angle sectors from Site B through the area define one direction of the fine sampling. Sample points are placed on the midlines so as to give the coarsest possible sample spacing that is still adequate to represent all sector equations. Each point of the finer grid is checked for consistency between the three ESM sites: if any site has detected no emitters in the sector containing the point, then the point is rejected. Otherwise, it defines a new variable in the equations.

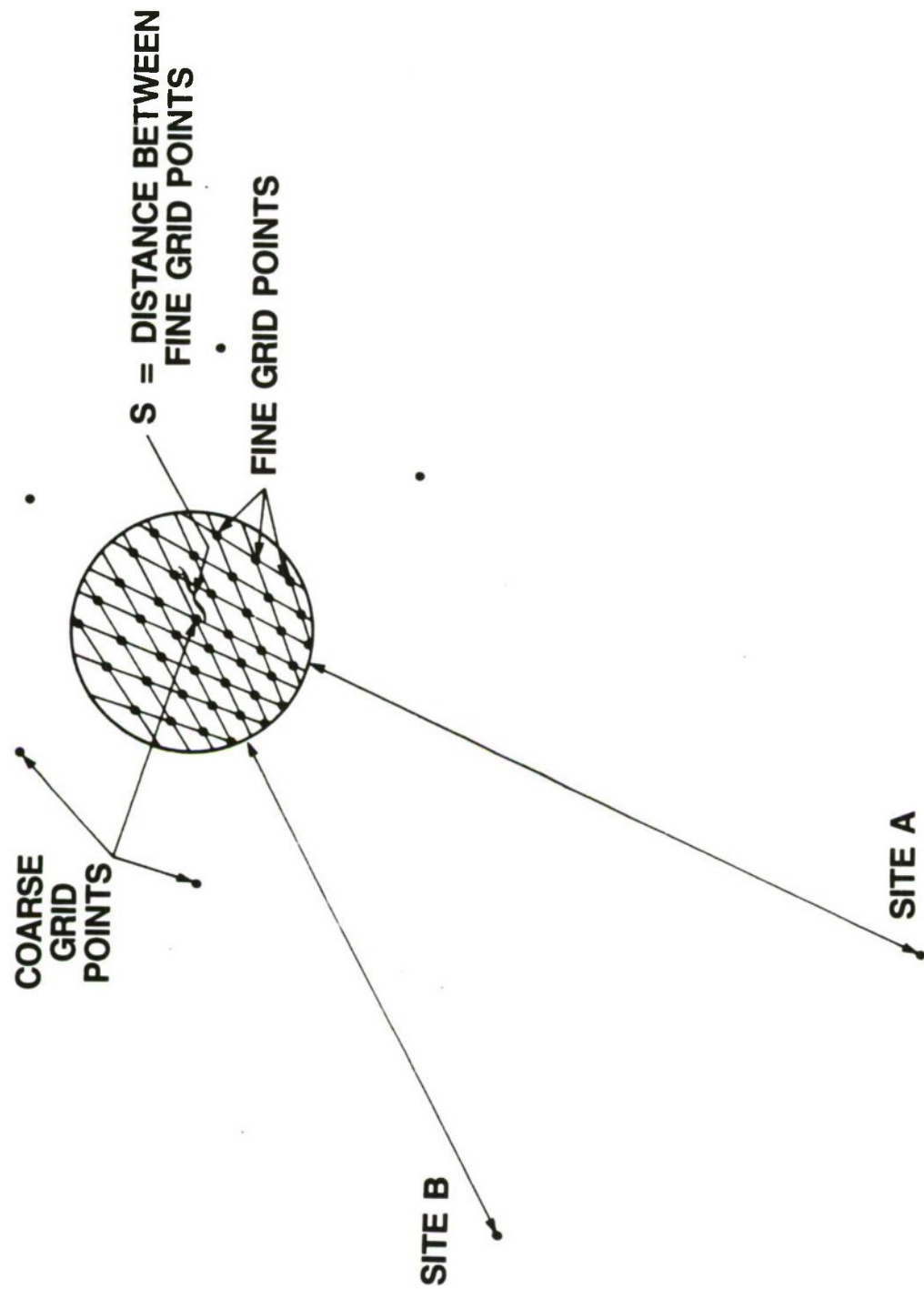


Figure 5. Sampling in Density Reconstruction



## SECTION 4

### TARGET DENSITY MAP EXAMPLES

In this section we look at two TDMs generated by the Target Density Reconstruction algorithm. Each TDM is an estimate using the same target locations as figure 1, so the ideal result would be a TDM as close as possible to figure 3. Angle measurement error was not modeled in this simulation, and an angle sector size of one degree was used. The stars in the figures show the locations of the three ESM sites.

Figure 6 shows a TDM generated on the assumption that the input ESM signal parameter data did not allow the signals to be sorted into subgroups for separate processing. This corresponds to the most difficult conditions for use of the Density Reconstruction algorithm. The figure shows that principal target groupings have been successfully reconstructed, although finer detail is missing, especially at points far from the ESM sites.

Figure 7 is a TDM generated on the more favorable assumption that the ESM systems could divide the signals into 14 subgroups for processing. With groups of up to 20 emitters, the Density Reconstruction algorithm was able to give a detailed picture of raid groupings. The TDM also accurately shows isolated small groupings of targets. As an area increases in size (e.g., 50 km by 50 km), the total estimated target count there gets closer to the true value. However, the estimated counts in an individual box within the area can differ significantly from the corresponding true value as given in figure 3.

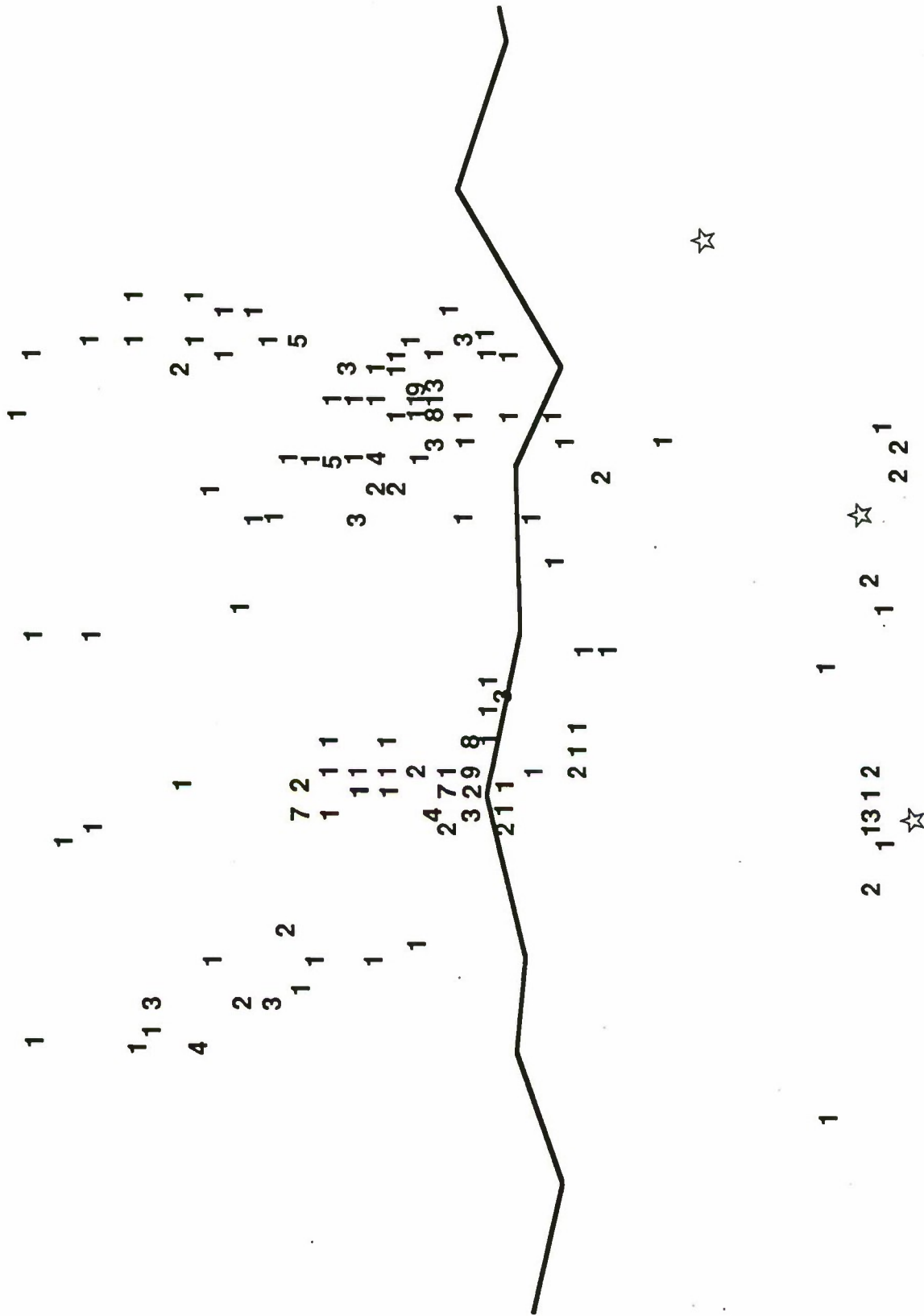


**Figure 6. Target Density Map: Reconstructed Densities**

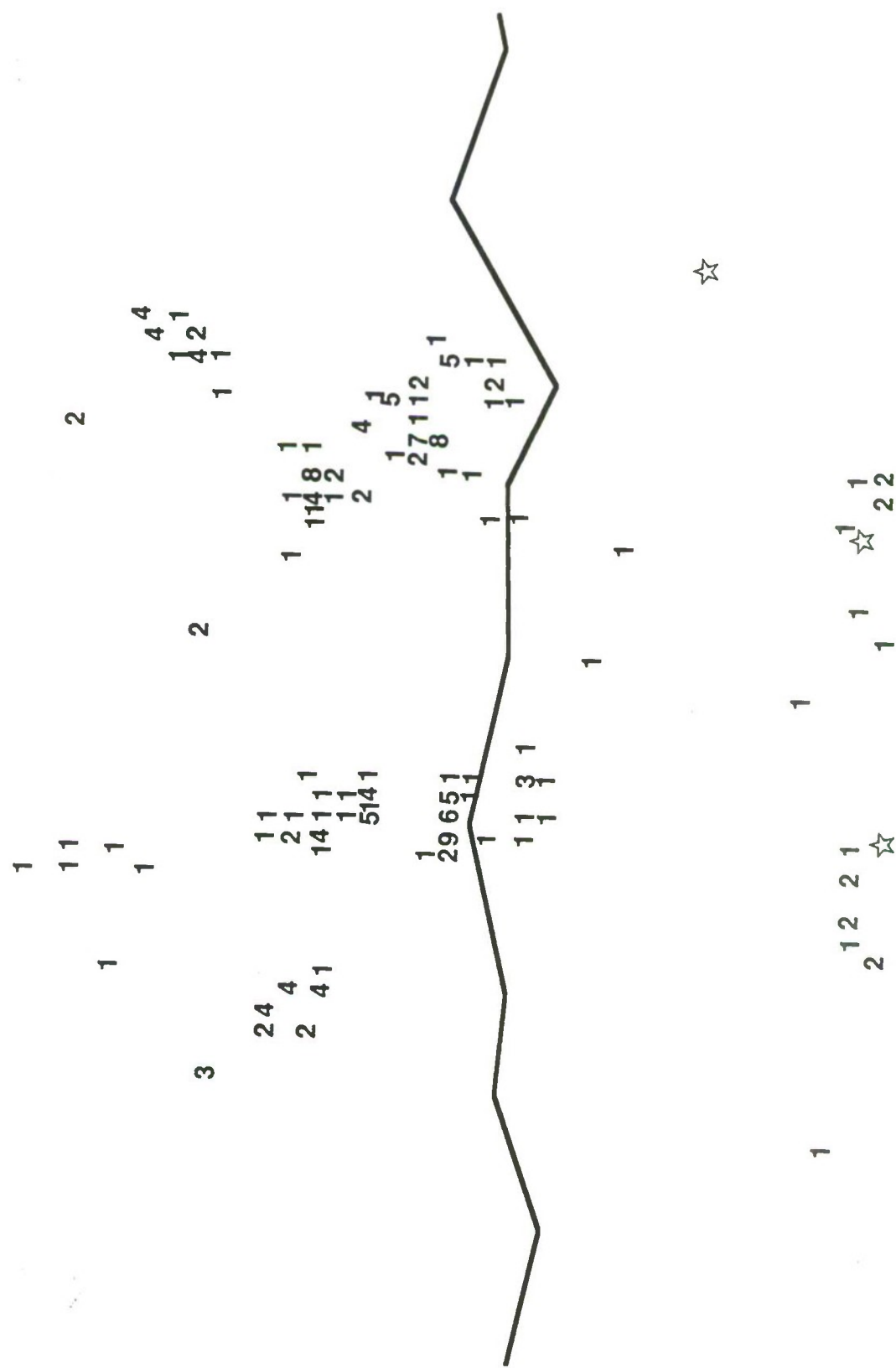


Figure 7. Target Density Map: Reconstructed Densities (9 Groups)

## SECTION 5

### CONCLUSION

We have presented a new method of using ESM angle and count data that generates an estimate of general raid target groupings. The information derived by the Target Density Reconstruction method and displayed on a Target Density Map makes the maximum possible use of the available input data.

The processing in Target Density Reconstruction is modeled on that in a CAT scanner, and has been adapted to the discrete target problem. The method uses a version of Maximal Entropy and the MENT algorithm to select a best TDM solution from the set of possible solutions.

Target Density Reconstruction could keep the user informed of major concentrations of air forces, and is intended as a backup in case primary radar is degraded, and if other sources such as ESM cooperative passive tracking are not available.

#### LIST OF REFERENCES

1. Hart, T., "An ESM Data Fusion Process for Tracking Mass Raids," Proceedings, Second Annual Tri-Service Data Fusion Symposium (1988).
2. Censor, Y., "Finite Series-Expansion Reconstruction Methods," Proc. IEEE, Vol. 71, No. 3, March 1983, pp. 409-419.
3. Herman, G., Image Reconstruction From Projections, New York: Academic Press, 1980.
4. Minerbo, G., J. Sanderson, "Reconstruction of a Source from a Few (2 or 3) Projections," Los Alamos Scientific Laboratory Informal Report LA-6747-MS, March 1977.
5. Jaynes, E. T., "On the Rationale of Maximum-Entropy Methods," Proc. IEEE, Vol. 70, No. 9, September 1982, pp. 939-952.
6. Minerbo, G., "MENT: A Maximum Entropy Algorithm for Reconstructing a Source from Projection Data," Computer Graphics and Image Processing, Vol. 10, 1979, pp. 48-68.